

Atomic Force Microscopy for Teaching Polymer Crystals and Polymer Blends

Maksim Dolmat,^{*§} Veronika Kozlovskaya, and Eugenia Kharlampieva^{*§}



Cite This: *J. Chem. Educ.* 2023, 100, 4047–4055



Read Online

ACCESS |

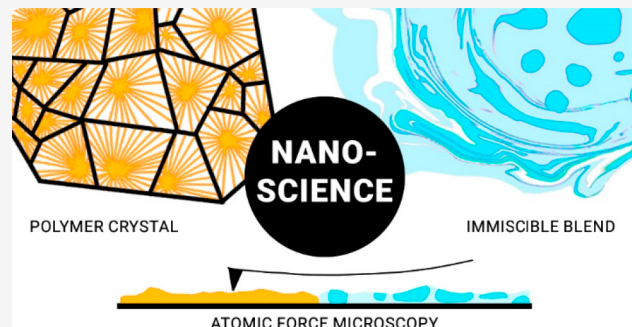
Metrics & More

Article Recommendations

Supporting Information

ABSTRACT: The essential component of expanding an undergraduate curriculum is the inclusion of lab experiments in nanoscience and nanomaterials, which significantly impact health and the environment through their use in food, cosmetics, agriculture, and medicine. We designed a laboratory experiment based on the atomic force microscopy (AFM) analysis of the physical characteristics of polymer blends and crystals, including surface morphology, Young's modulus, deformation, and stiffness. The laboratory exercise exposes students to the main aspects of the crystallization of polyethylene glycol and the formation of an immiscible polystyrene/polybutadiene blend, followed by optical microscopy and AFM characterization. In addition to providing information about the surface morphology and microstructure of the samples through AFM topography scanning, nanoindentation measurements allow for the mechanical characterization of materials with nanoscale resolution. Mechanical characterization offers students a broader application area where they can use their chemical understanding to regulate the material's physical characteristics. AFM force curve mapping enables assessment of the components' distribution in composite materials while analyzing each constituent independently with nanoscale precision. The versatility of AFM considerably increases the number of laboratory experiments that can be developed in undergraduate courses on nanoscience and nanomaterials. The knowledge acquired about polymer blending, crystallization, and their characterization at the nanoscale equips students with practical and transferable skills that they may apply in other chemistry and engineering classes to address real-world issues.

KEYWORDS: *Upper-Division Undergraduate, Graduate Education, Hands-on Learning, Polymer Chemistry, Laboratory Instruction, Atomic Force Microscopy*



INTRODUCTION

Nanoscience is an integral part of chemistry which describes materials with fundamentally novel features and properties at the nanoscale.¹ The National Nanotechnology Initiative² and the American Chemical Society³ emphasize the significance of developing innovative laboratory experiments^{4–8} and whole courses^{9–12} on nanomaterials and nanotechnologies to broaden the teaching of nanoscience. For instance, polymer crystals and blends exhibit unique nanostructures that give rise to specific macroscale properties and have applications in electrical devices, membrane materials, biomedical products, and food packaging.^{13,14} Polymer blends and polymer crystals are different from homogeneous materials like gels and glass, and their unique nanoscale features can be explored with analytical techniques accessible to undergraduate students.

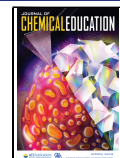
Atomic force microscopy (AFM) is one of the most prominent analytical techniques used for the nanoscale characterization of polymeric materials. The AFM laboratory experiment described here offers students the opportunity to learn about the modern state of nanoscience by combining the synthesis and nanoscale characterization of these polymeric materials.

The importance of polymeric nanostructured materials in modern technology highlights the need for corresponding laboratory modules.² The micro- and nanostructure of a polymer material significantly influences the macroscale physical properties, including toughness, mechanical strength, ductility, wear resistance, etc.¹⁶ AFM introduces students to the characterization of polymer materials at the nanoscale level as it measures a range of material characteristics such as surface morphology, roughness, elasticity, stiffness, and surface adhesion.^{17–19} For instance, in previous reports, students were introduced to nanoscale-resolution topography imaging for surface characterization of various materials, including polyvinylpyrrolidone films,²⁰ silver wires,²¹ gold nanoparticles,²² and dewaxed tomato cuticles.²³ Force curves obtained

Received: June 7, 2023

Revised: August 10, 2023

Published: September 15, 2023



by AFM nanoindentation were used to familiarize students with quantifying elastomer stiffness,²⁴ examining the connection between surface functionalization and adhesion forces,²⁵ and determining the attractive–repulsive forces of optical storage discs.²⁶ Our work bridges the gap between the macro- and nanoscale observations of polymer materials with distinctive surface topographies and highlights the AFM's nanoscale resolution capabilities. In addition, our approach allows the integration of surface topography imaging and force curve mapping to enable the quantitative analysis of Young's modulus, deformation, and stiffness in nonhomogeneous polymeric materials.

Students are introduced to different modes of AFM operation: tapping mode for topography images and contact mode for force measurements. In tapping mode, the AFM cantilever oscillates near its resonance frequency, maintaining a constant interaction with the sample surface. Scans are possible on various surfaces including soft samples. Contact mode measures the tip–sample interaction force as cantilever deflections are detected using a photodiode. Both modes use a feedback loop to enable constant interaction forces during scanning of high-resolution images. Tapping mode benefits from reduced damaging lateral forces and allows for phase imaging. Phase contrast imaging relies on the dynamic mode to obtain contrast based on material properties. It involves measuring the phase shift between the drive and response of an excited cantilever, which changes when there is a shift in the cantilever–sample interaction due to variations in material properties, providing crucial composition information for polymer blends.

Immiscible polymer blends are among the most popular heterogeneous polymer materials. A polymer blend is a mixture of two or more polymers with physical properties different from the initial polymers.^{12,15} Styrene–butadiene rubber is a prominent example of immiscible blends, consisting of two immiscible components and extensively utilized in manufacturing car tires.²⁷ Introducing polymer miscibility and blending to students allows their exploration of novel approaches for creating polymer materials with synergistic properties.²⁸ Previously, differential scanning calorimetry (DSC) was demonstrated to help teach students about the thermal transitions and compatibility of polymer blends.²⁹ Importantly, immiscible blends produce separate phases resulting in a heterogeneous mixture at a micrometer or nanometer scale.³⁰ Sadri et al. showcased the significance of polymer blending for its properties by examining its morphology with scanning electron microscopy and evaluating the tensile strength of various plastic wastes after recycling.³¹ Unlike previous experiments focused on evaluating the bulk physical characteristics of polymer blends, this laboratory experiment employs AFM to analyze the nanostructure of immiscible blends and assesses the mechanical properties of individual phases within the heterogeneous material on the nanoscale.

Polymer crystals are another class of polymer materials with a hierarchical nanostructure. Polymer crystals have a precise atomic and molecular arrangement, forming nanometer-range lamellae and spherical crystals with radii in the tens of micrometers, providing durability and superior performance in bearing, structural stress, and wear applications.^{32–35} In previous reports, students were introduced to polymer crystallization and its characterization through polarized-light microscopy to examine crystallization rates of poly(ethylene glycol) (PEG),³⁶ rapid scanning rate DSC with semicrystalline

polymers,³⁷ or Fourier transform infrared spectroscopy (FTIR) for Nylon 66's crystallinity.³⁸ Nonetheless, little focus has been on educating students about the morphological characteristics of polymer crystals on the nanoscale.

Herein, the inquiry-based laboratory exercise provides students with practical experience synthesizing and characterizing polymer crystals and blends using AFM. Through AFM characterization, students analyze materials with nanoscale surface morphologies not previously described in an educational context, while mechanical characterization of polymer blends using force curve mapping enables the assessment of the physical characteristics of individual components at the nanoscale. Discussing the structure–property relationship of polymer blends during AFM measurements of mechanical properties encourages students' chemical thinking, allowing them to predict and control the properties and behavior of polymer materials. This laboratory activity enables students to explore a range of concepts in polymer, materials, and nanotechnology sciences and may be easily integrated into courses covering introductory, analytical, and polymer chemistries as well as materials and nanotechnology science and engineering.

EXPERIMENTAL OVERVIEW

The polymer blends' phase separation and the disorganized melt's transformation to an ordered phase in linear chain polymers are investigated in an experiment implemented in the polymer chemistry laboratories for undergraduate and graduate students over four semesters. The described laboratory experiment involves a 20 min presentation outlining the experiment's details, 30 min of sample preparation, 15 min per group for optical microscopy analysis, and 30 min per group for AFM analysis. The experiment can be completed in one continuous laboratory session or divided into multiple sessions, with a total run time of around 3 h, depending on the number of groups. The University of Alabama at Birmingham's (UAB) Canvas learning management system (LMS) is used to publish the experiment's instructions and supporting materials online in advance. Since the course includes undergraduate and graduate students, one graduate student is typically partnered with two undergraduate students and students prepare samples in groups of three. However, two-person teams or individuals effectively completed the sample preparation and characterization. The first step of the experiment is sample preparation, where students prepare PS/polybutadiene (PB) blends and PEG crystals. Each group is assigned a certain PS/PB ratio and a certain PEG crystallization temperature. The Supporting Information (see SI-E) contains a complete description of the sample preparation process. Briefly, students are provided with stock solutions of PS (0.25 g/mL) and PB (0.25 g/mL) in toluene for the polymer blend samples. Students mix stock solutions with various PS/PB weight ratios in a scintillation vial. Students then prepare two samples for (1) optical microscopy by putting a drop of a blend solution on a clean, dry glass slide and covering it with a glass cover and (2) atomic force microscopy (AFM) by putting a drop of a blend solution on a clean, dry silicon wafer. To prepare an AFM sample of polymer crystals, students heat a silicon wafer to 60 °C on a hot plate. Then they add 5 mg of PEG to the silicon wafer, allow it to melt, and smear it into a thin film. The silicon wafers are then removed from the hot plate and allowed to cool under controlled conditions (at room temperature, in the freezer, or on a hot plate). Students prepare the sample for optical

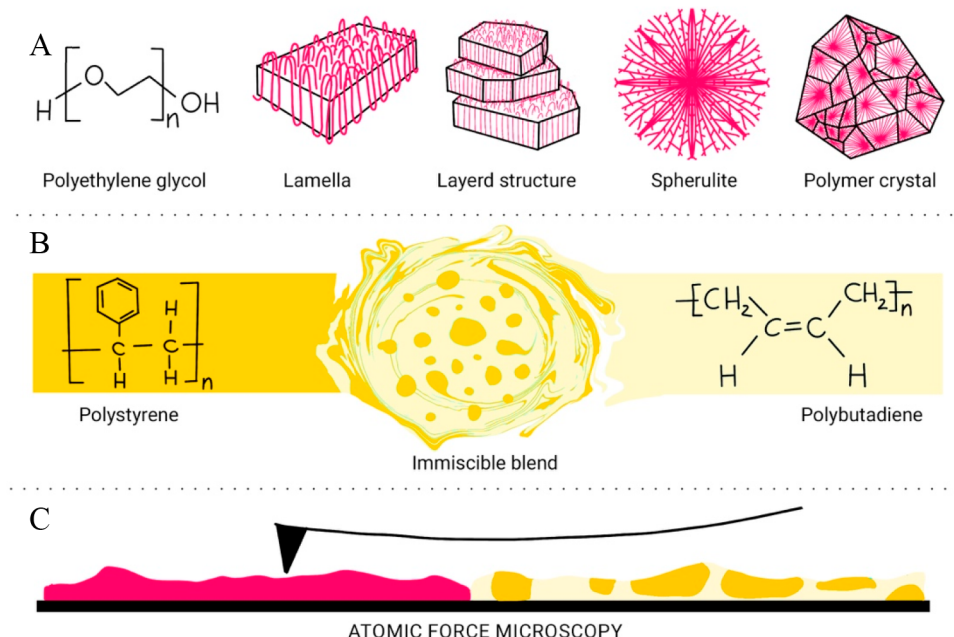


Figure 1. Schematic illustration of the laboratory experiment. Students first synthesize polymer crystals (A) and polymer blends (B), which are then analyzed by using atomic force microscopy (C).

microscopy using PEG mixed with an erythrosine B coloring dye. Students heat a glass slide on a hot plate to 60 °C. They then add approximately 5 mg of PEG/dye, allow it to melt, and spread it out with a covering glass.

Once samples are prepared, students use an optical microscope to measure the size of the generated spherulites and the polymer domains formed in polymer blends. The use of conventional optical microscopes rather than polarized-light microscopes is made possible by adding red coloring dye to PEG making spherulites visible to the naked eye. The NIH ImageJ³⁹ software is used to quantitatively analyze (a) the average diameters of the spherulites produced via various crystallization temperatures and (b) the average size of domains in polymer blends (see *SI-ImageJ* for the ImageJ User Guide). Both polymer crystals and blends were subjected to AFM topography and phase imaging to introduce students to surface morphology, roughness, and composition analysis. At the same time, nanoindentation measurements were carried out on polymer blends to demonstrate quantitative characterization of the local mechanical properties of the material. Topography AFM imaging and force–volume mapping of polymer blends and crystals were conducted using an AFM instrument (NT-MDT Spectrum Instruments) with an SPM system controller. The imaging and nanoindentation measurements were performed using sharp pyramidal NSG30 probes (tip curvature radius < 10 nm; cantilever length, 125 μm; cantilever width, 40 μm; cantilever thickness, 3.5–4.5 μm; resonance frequency ~ 260 kHz; force constant, 22–100 N m⁻¹) purchased from NT-MDT Spectrum Instruments. The acquired data were analyzed using the NT-MDT image processing and analysis software. Groups can be combined into larger groups (5–6 students per group) to complete AFM scanning in a single laboratory session, or each group can run its samples independently to allow every student to practice scanning techniques. Students present their conclusions using the analyzed data after completing the laboratory activities. During the Q&A session, students' understanding of the

observed effect is evaluated, with most of the questions related to the topics of (1) crystallization and the impact of temperature on the size of spherulites, (2) the polymer blends and their properties, and (3) the main concepts of optical microscopy and AFM. The general knowledge and practical information learned throughout the experiment are assessed on the final exam.

■ HAZARDS

Polystyrene (PS), poly(ethylene glycol) (PEG), and polybutadiene (PB) are classified as nonhazardous. Avoid breathing any polymer dust that could be present. There is a risk associated with using a hot plate. Use tweezers when handling hot glass slides. Used microscope slides that contain PEG crystals or polymer blends should be disposed of in a glass-waste container. PEG, PS, and PB can be disposed of in regular trash, while glass containers for organic waste should be used to dispose of polymer solutions. Toluene is flammable and can irritate the skin when inhaled, ingested, or absorbed in the skin. Erythrosine B is classified as an irritant that can create a burning sensation or rash when it comes into contact with the skin.

■ RESULTS AND DISCUSSION

Polymer Crystals

Figure 1A summarizes the main steps of polymer crystallization. Each polymer molecule folds up on itself in an accordion-style manner to accommodate its extraordinary length within the crystal, generating what is called a lamella.⁴⁰ From the initial nucleus, individual ribbon-like lamellae spread outward in all directions, forming a layered structure. The lamellae continuously branch out and fan out until the ultimate crystal structure, known as spherulite, is obtained.⁴¹ Panels A–C of Figure 2 show the student-fabricated spherulites with well-defined circular profiles that were produced at different crystallization temperatures. While a polarized-light optical microscope is typically used to observe the spherulite

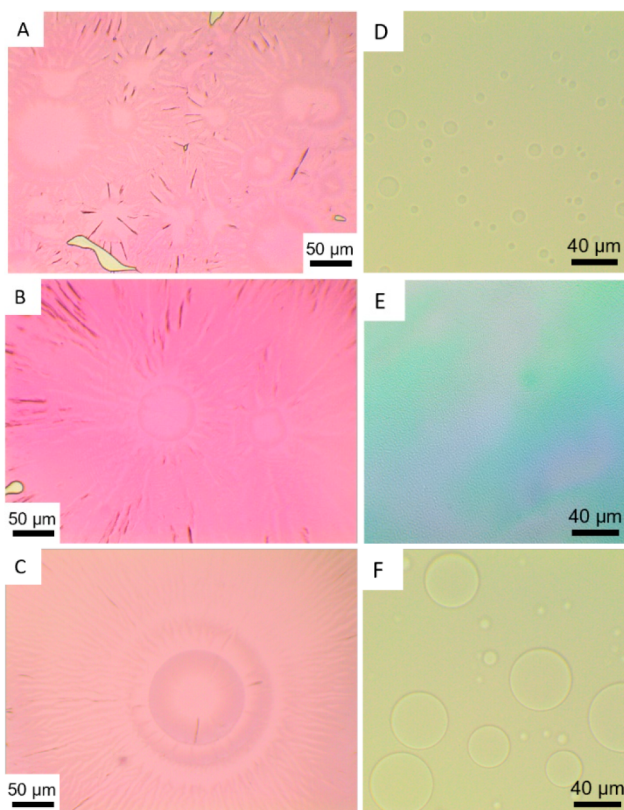


Figure 2. Optical micrographs of PEG spherulites synthesized by cooling at $-18\text{ }^{\circ}\text{C}$ (A), room temperature (B), and gradual cooling from $60\text{ }^{\circ}\text{C}$ to room temperature on a hot plate (C). (D–F) Optical micrographs of PS/PB blends synthesized at mixture ratios 90/10 (D), 70/30 (E), and 30/70 (wt %) (F).

structures, adding a coloring dye to PEG powder enables viewing the crystals with a typical optical microscope, making this work more widely accessible, since conventional microscopes are much more affordable than polarizing ones. Students can determine the spherulite radial distance from optical micrographs by adding a scale bar and doing image analysis in ImageJ software or by utilizing the software of the optical microscope. **SI-ImageJ** provides a detailed tutorial on the ImageJ software. The polymer spherulites' radial growth rate is constant at constant pressure and temperature.³⁶ However, the rate of polymer crystallization varies at different cooling rates. As a result, samples left on a hot plate have the lowest crystallization rate, resulting in the largest homogeneous spherulites with no defects and few amorphous regions. Conversely, a rapid change in the crystallization temperature leads to an increase in the number of crystallization centers and a faster rate of spherulite formation, which result in defects and amorphous zones.

AFM is employed to obtain additional lamellar data from PEG spherulites. Compared to an optical microscope, AFM has a more than 1000 times greater resolution, enabling students to characterize the crystal morphology in detail. Figure 3 illustrate AFM topography images of PEG crystals, which show the spherulites' surface morphology and microstructure. When looking at the typical spherulite, one can see the parallel growth of lamellae. AFM enables the acquisition of high-resolution images on a $1\text{ }\mu\text{m}^2$ region, providing the surface roughness and the lamella's average width and height. The roughness was calculated as the root-mean-square (RMS)

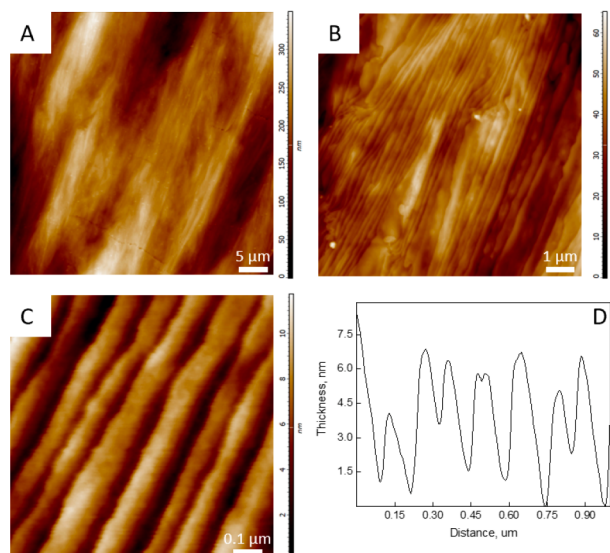


Figure 3. AFM topography images of PEG spherulites synthesized by cooling at room temperature over 50 (a), 10 (b), and 1 (c) μm^2 areas. (D) Section profile of the lamella structures.

value and determined to be $2.8 \pm 0.4\text{ nm}$. Students were also instructed on creating cross-sectional profiles of the lamella using image processing software; an example of a student-created cross-sectional profile is given in Figure 3D. Using section profiles, students determined lamellae's average width of $87 \pm 20\text{ nm}$ and height of $5 \pm 1\text{ nm}$.

In this portion of the lab exercise, students learn about polymer crystallization and the impact of the temperature on polymer crystal growth. Students used an optical microscope and an AFM to characterize the crystal samples. Students gain practical experience in sample preparation and material characterization. The students used the optical microscope with great enthusiasm, as it allowed for the fast confirmation of crystal formation. Although numerous complicated designs strive to increase the optical micrographs' resolution and sample contrast, basic optical microscopes are relatively straightforward, providing each group with practical experience. Because optical microscopes employ visible light and allow for direct visual observation of the material, they have historically been widely used in science, making them essential for undergraduate courses. Analysis of the average size of the spherulites exposes students to ImageJ software, which is widely used in the biomedical and engineering fields. Significantly, students experience using an atomic force microscope firsthand. After acquiring all of the data, which involved hands-on scanning under instructor supervision and subsequent discussions, students demonstrated a comprehensive understanding of AFM fundamentals, scanning procedures, and processing of AFM images. Students found the ability of AFM to scan defined features of spherulites to be fascinating, especially when it could provide a 3D image rendering.

Polymer Blends

This laboratory activity examines mixtures of polymers with known ratios of immiscible PS/PB blends. Drop-casting was used to deposit PS/PB blend films on glass and silicon substrates, which were analyzed using a standard optical microscope and AFM. PS and PB polymers were selected due to their immiscibility and significant difference in mechanical

characteristics. An optical microscope can quickly confirm the formation of a polymer blend. The PS/PB blend film forms circular droplets that range in diameter from 20 to 50 μm (Figure 2D–F). Circular droplets originate from the reduction of the polymer domain's surface area in contact with the underlying substrate, and those caused by blend incompatibility inside the drop. Using the bright-field imaging method, the students investigated the microphase separation in PS/PB blends with various blend ratios. The blend ratio significantly impacts the domain size and phase-separated morphology of PS/PB, as shown in Figure 2D–F. In the 90/10 (wt %) PS/PB blend, the PS component predominates as a continuous phase, while small, circular domains of PB separate from the PS phase. The isolated PB spheres tend to consolidate into larger domains as the proportion of PB increases to 30 wt %, leading to irregular domain structures forming a bicontinuous transition phase.⁴² If the amount of PB is increased even further, to 70 wt %, the morphology is inverted, with PS becoming a minor component with the small spherical PS domains contained in the PB matrix. The average size of the PS domains gradually decreases as the content of PB progressively rises from 50 to 70 wt %.

Students prepare an AFM sample of a PS/PB blend by drop-casting the polymer mixture on a silicon wafer. Both topography and nanoindentation analyses were used to analyze the PS/PB blends, demonstrating the advantages and versatility of AFM. AFM enables the simultaneous capture of spatial maps of material composition and surface topography with nanometer precision.⁴³ A 50 μm^2 topographic image and the matching phase shift map collected in the dynamic mode are shown in Figure 4. Students note the blend's typical

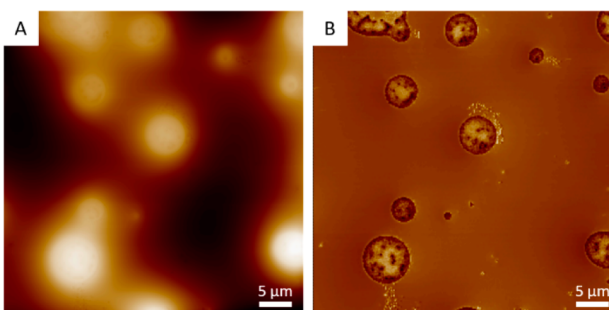


Figure 4. AFM topography (A) and phase (B) images of PS/PB blends synthesized at mixture ratio 90/10 (wt %). Z-scale is 600 nm.

morphology, with domains of different sizes (higher regions) spread throughout the matrix (lower regions). While the smaller domains are circular, the larger domains—formed by joining several round domains—can have an irregular shape. A phase shift image can be used to differentiate between two or more materials, but it cannot provide precise data on their physical characteristics. The cantilever's resonance frequency undergoes a shift when there are changes in the cantilever–sample interaction, such as variations in material properties. Consequently, brighter regions indicate stiffer materials in a typical phase image, while darker areas indicate softer materials. Thus, students can observe the distribution of the polymer domains in the phase shift maps and the material difference between PB and PS (Figure 4B). Based on the composition used for the AFM analysis, 90/10 (wt %) PS/PB, students know that PS is the matrix and the domains are PB. Force–distance curve mapping was employed to acquire

quantitative data on the mechanical characteristics of the sample and provide Young's modulus, deformation, stiffness, and adhesion data.

By indenting a sample surface, obtained force–distance curves enable quantitative assessment of a material's physical and mechanical characteristics, including Young's modulus, deformation, and adhesion. The concept of force–distance curves is discussed with students. Figure 5 illustrates a single

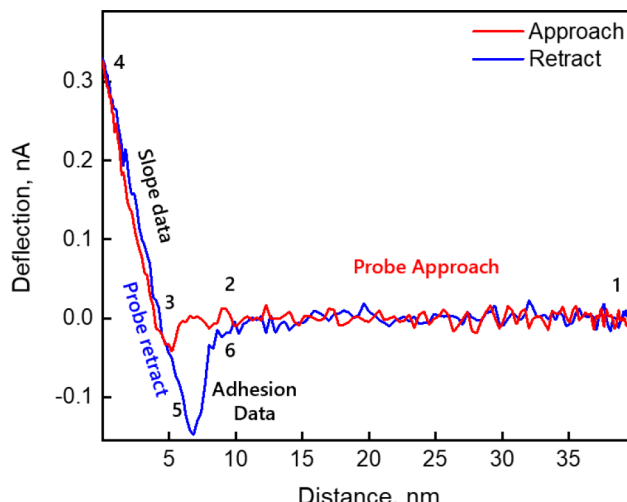


Figure 5. AFM approaching (red) and retractive (blue) force–distance curves obtained for PS part of PS/PB blend synthesized at mixture ratio 90/10 (wt %).

force–distance curve in approach and retraction modes that plot tip–sample force against piezo movement. The distance between the surface and the tip is shown on the x -axis. Region 1–2 represents the area where the tip moves toward the probe, indicating that the tip is not in contact with the sample's surface. A small dip is observed at point 3 on the approach curve (red curve), indicating the AFM tip's "snap into contact" with the sample due to tip–surface interactions, such as capillary forces. Region 3–4 displays the cantilever's deflection as it comes into contact with the sample surface, where repulsive van der Waals interactions exist between the tip and sample, resulting in cantilever deflection. The slope in this linear region is inversely proportional to surface stiffness, and while for infinitely rigid substrates, the slope is 1 (indicating no sample deformation), in our case, on the polystyrene surface, the slope differs from 1 due to both sample and cantilever deformation. This region can become nonlinear due to plastic deformation, viscoelasticity, and non-uniform surface deformation. The tip retraction commences at point 4 (Region 4–5) as the maximum force is reached, with the tip unbending while being withdrawn from the surface. Ideally, for purely elastic deformation, lines 3–4 and 4–5 should overlap with the same slope for the approaching (red) and retracting (blue) curves. The minimum on the repulsive portion (point 5 on the blue curve) signifies the point with the strongest, attractive van der Waals interactions between the tip and sample. The area between lines 5 and 6 represents the adhesion force required to separate the two surfaces.

A two-dimensional (2D) map of the material's physical characteristics can be generated by compiling a collection of force–distance curves with a few-nanometer precision by using a sharp tip. In this experiment, students utilize the NT-MDT

Hybrid (HD) mode to perform mechanical property mapping, acquiring ~65000 force curves to examine the spatial distribution within the scanned region. The HD mode allows high-resolution local adhesion and stiffness mapping, enhancing AFM compositional mapping through quantitative analysis of the local mechanical properties. By intermittently contacting the probe and sample in the vertical direction and using the resulting probe deflection for surface tracking feedback, nanoscale structures are visualized and multiple mechanical parameters such as Young's modulus, deformation, and stiffness are simultaneously acquired, offering a comprehensive understanding of the blend's mechanical behavior. The scanning area was chosen to include both PB domains and the PS matrix so students can see the difference in mechanical characteristics between the materials. Figure 6 demonstrates topography (A), Young's modulus (B), deformation (C), and stiffness (D) maps of PS/PB blends synthesized at a mixture ratio of 90/10 (wt %).

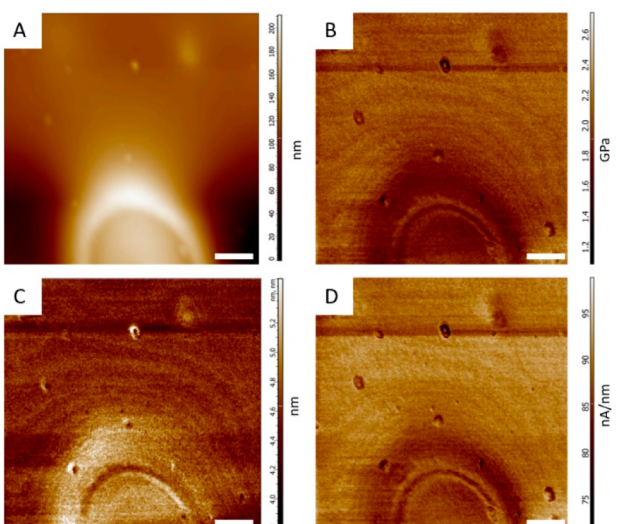


Figure 6. AFM topography (a), Young's modulus (b), deformation (c), and stiffness (d) maps of PS/PB blends synthesized at mixture ratio 90/10 (wt %). Scale bar: 1 μ m.

Young's modulus provides information about when a material will break or bend by measuring a material's capacity for stretching and deformation. The distribution of Young's modulus over the PS/PB blend is shown in Figure 6B. Students can observe the difference in the distribution of Young's modulus throughout the map, which has lower (dark areas) and higher (bright areas) values. While there is a noticeable difference between PS (matrix) and PB (domains) in terms of Young's modulus, the gathered maps show students the uniform distribution of Young's modulus values among single component materials. Students' analysis of Young's modulus maps demonstrated that PS has an average Young's modulus of 2 ± 0.1 GPa, which agrees with the literature data.⁴³ Similarly, students utilized force–volume mapping to quantify the Young's modulus of PB domains, determining an average value of approximately 1.7 ± 0.1 GPa. While literature values for homogeneous PB indicate a range of 3–8 MPa,⁴⁴ it is essential to note that polybutadiene is susceptible to oxidation when exposed to air at room temperature due to the presence of numerous carbon double bonds in its molecules.⁴⁵ A previous study has demonstrated a significant increase in

Young's modulus of PB with prolonged exposure to air, with values varying from an initial 3.6 ± 0.4 to 1400 ± 150 MPa after 625 h of exposure.⁴³ Since the students prepared their samples in advance and left them exposed to air for 1 week, the recorded Young's modulus falls within the GPa range and agrees with previously reported data.

AFM nanoindentation allows for material deformation in the nanoscale range and can be used on various materials, including soft biomaterials and thin film coatings. Young's modulus and deformation data are simultaneously gathered and calculated from force–distance curves, allowing for the construction of a 2D map of the sample's deformation (Figure 6C). Deformation refers to the sample's response to the maximum applied force. It represents the variance between the piezo displacement and the cantilever bending, expressed in nanometers at the maximum force. Lesser Young's modulus values correspond to a higher material's deformation, and higher Young's modulus values correspond to a lower material's deformation. The deformation and Young's modulus maps can be used as visual aids to illustrate this correlation. The blend's Young's modulus map reveals that PS has greater values (bright regions) than PB (darker areas), yet the deformation map is presented reversely, with brighter areas for PB and darker areas for PS. Quantitative data can be retrieved from these maps, showing that the deformation of PB is 5.1 ± 0.1 nm compared to 4.4 ± 0.1 nm for PS.

Finally, AFM may be used as a nanoindenter to determine the sample's stiffness. Stiffness relates to the material's capacity to withstand external pressure and regain its original shape upon removal of external force. A material's stiffness and elasticity, or flexibility, are firmly connected, and a material with a lower stiffness is more flexible. Students may associate the deformation of PS and PB with matching stiffness from the gathered maps (Figure 6D) since the material's deformation defines flexibility. The stiffness map, quantified in nA/nm, is utilized for visualization and enhanced contrast, surpassing the Young's modulus map. It proves valuable for qualitative comparison of mechanical properties among different polymer blend components. Higher PB deformation results in lower material stiffness; on the contrary, lower PS deformation results in greater material stiffness. Specifically, the PS stiffness calculated by the students was 0.09 nA/nm. However, the reported stiffness corresponds to the slope of the as-measured force curve without considering the inverse optical lever sensitivity and the cantilever spring constant. For precise quantitative characterization, stiffness should be converted to N/m (see the experimental part for detailed calculations).

Due to time constraints in the laboratory course, students could collect the topography, Young's modulus, deformation, and stiffness data for the PS/PB blends synthesized at a mixture ratio of 90/10 (wt %). However, to broaden the laboratory experiment and enhance the learning objectives, it is recommended to include a second data set for a 30/70 (wt %; PS/PB) sample in parallel to the 90/10 (wt %) sample. This additional data set would offer a flipped identity of the matrix and domains, making it more evident that the higher deformation, consequently lower Young's modulus and stiffness, of the PB is conserved, even when PB serves as the matrix.

Ultimately, by working with polymer blends, students learn how the ratio of polymers can change a polymer blend's morphology, causing one phase to be a continuous matrix and another to be a domain. Students learn the fundamentals of

polymer blends and how to characterize them with an optical microscope and AFM. ImageJ can be used to evaluate the domains' average sizes, boosting the learning experience for students working with previously unfamiliar software. Students obtain a foundational understanding of the AFM nano-indentation method while refreshing their expertise in topographical imaging that they previously acquired through polymer crystal scanning. Students completed the laboratory experiment and showed a thorough understanding of force-distance curves and the assessment of the mechanical characteristics of materials.

Evaluation of Students' Performance

Following the lab experiment, the students produce a laboratory report in the form of a presentation that highlights the key learning points:

- polymer crystals and their applications
- polymer blends and their properties
- principles and applications of optical microscopy
- principles and capabilities of AFM

Completing a final report as a presentation is an effective way to learn through teaching that enhances general understanding and information retention. Students' ability to seek relevant literature and self-educate on the primary subject of the presented lab activity improved as a result of presentation preparation. This laboratory activity enables thorough learning from various perspectives, including learning by hearing during an introductory lecture, learning through a hands-on experiment, and learning by teaching during a presentation. Additionally, students develop their communication skills by making concise, clear, and insightful presentations. Allowing students to present their work in a template-free format empowers their creativity, enhancing their peers' education in a way that piques their interest and attention during presentations. Students collaboratively collect, analyze, and present data as a group during the experiment. The groups are assigned different sample preparation conditions, leading to postpresentation discussions where they compare results and explain discrepancies and sample-specific characteristics. Students are given a general presentation outline covering the introduction/background, hypothesis, experiment details, data analysis, and conclusions, and they receive the presentation evaluation rubric beforehand to assist in their preparation.

After completing the assignment, students showed a thorough understanding of polymer blends, crystals, and the techniques for their characterization, such as an optical microscope and AFM. This experiment has been carried out over the past four semesters as a component of the polymer chemistry laboratory course for undergraduate and graduate students. The presentation served as a practice tool to evaluate students' knowledge and comprehension of the subject. Additionally, the final test included questions from the Supporting Information (SI-Q) to gauge the understanding of the experiment.

CONCLUSIONS

We designed a laboratory exercise for AFM analysis of polymer blends and crystals, adding to the library of chemistry experiments that is accessible for undergraduate nanoscience courses. By collecting the physical properties of the samples, including surface morphology and mechanical characteristics of the polymer blends and crystals, at the nanoscale, the described

experiment introduces essential fundamental concepts of nanostructured polymeric materials. Students obtain hands-on experience synthesizing polymer blends and crystals and using optical microscopy to confirm the formation of spherulites and immiscible blends. Students use ImageJ software to assess the average sizes of the spherulites and polymer domains in polymer blends. The following AFM characterization provides further information about the materials' nano- and microstructure. Student exposure to mechanical property characterization techniques provides them with a broader application area for utilizing their chemical expertise to control the material's physical properties. Students evaluate the distribution of constituents in composite materials and analyze each attribute separately with nanoscale-resolution AFM force curve maps. Using atomic force microscopy in undergraduate courses creates a wide range of new opportunities for property characterization at the nanoscale for various scientific and industrial applications. Ultimately, students explore a broad range of concepts in polymer, materials, and nanotechnology sciences, which combines fundamental knowledge of generally new topics for undergraduate curricula, polymer blends, and crystals, while gaining practical experience with AFM. Acquired knowledge and skills can be applied practically or transferred to other courses.

ASSOCIATED CONTENT

Supporting Information

The Supporting Information is available at <https://pubs.acs.org/doi/10.1021/acs.jchemed.3c00545>.

Samples of final exam questions ([PDF, DOCX](#))

Detailed experimental sections of synthesis of polymer crystals and polymer blends ([PDF, DOCX](#))

ImageJ user guide ([PDF, DOCX](#))

AUTHOR INFORMATION

Corresponding Authors

Maksim Dolmat – Department of Chemistry, The University of Alabama at Birmingham, Birmingham, Alabama 35294, United States;  orcid.org/0000-0002-4918-7342; Email: maksim@uab.edu

Eugenia Kharlampieva – Department of Chemistry and Center for Nanomaterials and Biointegration, The University of Alabama at Birmingham, Birmingham, Alabama 35294, United States;  orcid.org/0000-0003-0227-0920; Email: ekharlam@uab.edu

Author

Veronika Kozlovskaya – Department of Chemistry, The University of Alabama at Birmingham, Birmingham, Alabama 35294, United States;  orcid.org/0000-0001-9089-4842

Complete contact information is available at: <https://pubs.acs.org/10.1021/acs.jchemed.3c00545>

Author Contributions

[§]M.D. and E.K. have equal seniority.

Notes

The authors declare no competing financial interest.

ACKNOWLEDGMENTS

The authors thank Claire Thomas for helping to design and direct the class and all students who participated in this study. Technical assistance was provided by Dr. Aaron Alford (Chemistry Department, UAB). This work was supported by NSF DMR Award No. 1904816 and the UAB Department of Chemistry.

REFERENCES

- (1) Roco, M. From Vision to the Implementation of the U.S. National Nanotechnology Initiative. *J. Nanopart. Res.* **2001**, *3*, 5–11.
- (2) Roco, M. Converging Science and Technology at the Nanoscale: Opportunities for Education and Training. *Nat. Biotechnol.* **2003**, *21*, 1247–1249.
- (3) Wenzel, T. J.; McCoy, A. B.; Landis, C. R. An Overview of the Changes in the 2015 ACS Guidelines for Bachelor's Degree Programs. *J. Chem. Educ.* **2015**, *92* (6), 965–968.
- (4) Abu-Much, R. From Redox Reactions to Nanomaterials: Visual Lab Activity for Exploring the Stabilization and Aggregation of Silver Nanoparticles. *J. Chem. Educ.* **2021**, *98*, 4037–4045.
- (5) Rattanakit, P. Open Inquiry-Based Laboratory Project on Plant-Mediated Green Synthesis of Metal Nanoparticles and Their Potential Applications. *J. Chem. Educ.* **2021**, *98*, 3984–3991.
- (6) Orbaek, A. W.; McHale, M. M.; Barron, A. R. Synthesis and Characterization of Silver Nanoparticles for an Undergraduate Laboratory. *J. Chem. Educ.* **2015**, *92*, 339–344.
- (7) Strachan, J.; Barnett, C.; Maschmeyer, T.; Masters, A. F.; Motion, A.; Yuen, A. K. Nanoparticles for Undergraduates: Creation, Characterization, and Catalysis. *J. Chem. Educ.* **2020**, *97*, 4166–4172.
- (8) Dolmat, M.; Thomas, C.; Kozlovskaya, V.; Kharlampieva, E. Multivariate Polymer Laboratory on Synthesis of Alginate Hydrogel Beads and Analysis of Dye Loading and Release. *J. Chem. Educ.* **2022**, *99*, 3289–3297.
- (9) Park, E. J. Nanotechnology Course Designed for Non-Science Majors to Promote Critical Thinking and Integrative Learning Skills. *J. Chem. Educ.* **2019**, *96*, 1278–1282.
- (10) Blonder, R. The Story of Nanomaterials in Modern Technology: An Advanced Course for Chemistry Teachers. *J. Chem. Educ.* **2011**, *88*, 49–52.
- (11) Walters, K. A.; Bullen, H. A. Development of a Nanomaterials One-Week Intersession Course. *J. Chem. Educ.* **2008**, *85*, 1406.
- (12) Bauer, J. Teaching Nanotechnology through Research Proposals. *J. Chem. Educ.* **2021**, *98*, 2347–2355.
- (13) Nyamweya, N. N. Applications of Polymer Blends in Drug Delivery. *Future J. Pharm. Sci.* **2021**, *7*, 18.
- (14) Zhang, G.; Li, Q.; Allahyarov, E.; Li, Y.; Zhu, L. Polymer Nanodielectrics for Capacitive Energy Storage. *ACS Appl. Mater. Interfaces* **2021**, *13* (32), 37939–37960.
- (15) Gleiter, H. Nanostructured Materials: State of the Art and Perspectives. *Nanostruct. Mater.* **1995**, *6*, 3–14.
- (16) Banerjee, R.; Ray, S.; Ghosh, A. Microstructure Development and Its Influence on the Properties of Styrene-Ethylene-Butylene-Styrene/Polystyrene Blends. *Polymers* **2018**, *10*, 400.
- (17) Abbasi Moud, A. Cellulose Nanocrystals Examined by Atomic Force Microscopy: Applications and Fundamentals. *ACS Food Sci. Technol.* **2022**, *2* (12), 1789–1818.
- (18) Goss, J.; Volle, C. B. Using Atomic Force Microscopy to Illuminate the Biophysical Properties of Microbes. *ACS Appl. Bio Mater.* **2020**, *3* (1), 143–155.
- (19) Fukuma, T.; Garcia, R. Atomic- and Molecular-Resolution Mapping of Solid–Liquid Interfaces by 3D Atomic Force Microscopy. *ACS Nano* **2018**, *12* (12), 11785–11797.
- (20) Sanders, W. C. Fabrication of Polyvinylpyrrolidone Micro-/ Nanostructures Utilizing Microcontact Printing. *J. Chem. Educ.* **2015**, *92*, 1908–1912.
- (21) Sanders, W. C.; Ainsworth, P. D.; Archer, D. M.; Armajo, M. L.; Emerson, C. E.; Calara, J. V.; Dixon, M. L.; Lindsey, S. T.; Moore, H. J.; Swenson, J. D. Characterization of Micro- and Nanoscale Silver Wires Synthesized Using a Single-Replacement Reaction between Sputtered Copper Metal and Dilute Silver Nitrate Solutions. *J. Chem. Educ.* **2014**, *91*, 705–710.
- (22) Dungey, K. E.; Voss, E. J.; Wiediger, S. D. Counting Gold: Using Atomic Force Microscopy to Characterize Gold Nanoparticles. *J. Chem. Educ.* **2022**, *99*, 2684–2688.
- (23) Sarkar, S.; Chatterjee, S.; Medina, N.; Stark, R. E. Touring the Tomato: A Suite of Chemistry Laboratory Experiments. *J. Chem. Educ.* **2013**, *90*, 368–371.
- (24) Ferguson, M. A.; Kozlowski, J. J. Using AFM Force Curves to Explore Properties of Elastomers. *J. Chem. Educ.* **2013**, *90*, 364–367.
- (25) Trought, M.; Perrine, K. A. Investigating the Relationship between Adhesion Forces and Surface Functionalization Using Atomic Force Microscopy. *J. Chem. Educ.* **2021**, *98*, 1768–1775.
- (26) Bancroft, S. F.; Ali, M. A.; Kohli, P. An Inquiry-Based Introduction to Atomic Force Microscopy Techniques through Optical Storage Disc Surface Imaging. *J. Chem. Educ.* **2022**, *99*, 3030–3038.
- (27) Wang, Q.; Wang, W.; Li, Q.; Wu, C. Mechanically Robust and Recyclable Styrene–Butadiene Rubber Cross-Linked via Cu²⁺–Nitrogen Coordination Bond after a Tetrazine Click Reaction. *Ind. Eng. Chem. Res.* **2021**, *60* (5), 2163–2177.
- (28) Naseem, R.; Montalbano, G.; German, M. J.; Ferreira, A. M.; Gentile, P.; Dalgarno, K. Influence of PCL and Phbv on Plla Thermal and Mechanical Properties in Binary and Ternary Polymer Blends. *Molecules* **2022**, *27*, 7633.
- (29) Ploeger, R. Differential Scanning Calorimetry for Art Conservation Graduate Students: A Practical Laboratory Exercise Using Polymer Blends. *J. Chem. Educ.* **2018**, *95*, 1192–1197.
- (30) Prusty, D.; Pryamitsyn, V.; Olvera de la Cruz, M. Thermodynamics of Associative Polymer Blends. *Macromolecules* **2018**, *51*, 5918–5932.
- (31) Sadri, M.; Smith, P.; Spears, S.; Perkins, J.; Dewitt, C.; Savannah, S.; Butler, C.; Qiang, Z. Hands-on Laboratory Experiments for Demonstrating Mixed Plastic Recycling. *J. Chem. Educ.* **2023**, *100*, 321–326.
- (32) Lotz, B.; Miyoshi, T.; Cheng, S. Z. D. 50th Anniversary Perspective: Polymer Crystals and Crystallization: Personal Journeys in a Challenging Research Field. *Macromolecules* **2017**, *50*, 5995–6025.
- (33) Keller, A. Polymer Crystals. *Rep. Prog. Phys.* **1968**, *31*, 623–704.
- (34) Han, W.; Liao, X.; Yang, Q.; Li, G.; He, B.; Zhu, W.; Hao, Z. Crystallization and Morphological Transition of Poly(l-Lactide)–Poly(ϵ -Caprolactone) Diblock Copolymers with Different Block Length Ratios. *RSC Adv.* **2017**, *7*, 22515–22523.
- (35) Huang, S.; Jiang, S.; An, L.; Chen, X. Crystallization and morphology of poly(ethylene oxide-b-lactide) crystalline-crystalline diblock copolymers. *J. Polym. Sci., Part B: Polym. Phys.* **2008**, *46*, 1400–1411.
- (36) Singfield, K. L.; Chisholm, R. A.; King, T. L. A Physical Chemistry Experiment in Polymer Crystallization Kinetics. *J. Chem. Educ.* **2012**, *89*, 159–162.
- (37) Badrinarayanan, P.; Kessler, M. R. A Laboratory to Demonstrate the Effect of Thermal History on Semicrystalline Polymers Using Rapid Scanning Rate Differential Scanning Calorimetry. *J. Chem. Educ.* **2010**, *87*, 1396–1398.
- (38) Vasanthan, N. Crystallinity Determination of Nylon 66 by Density Measurement and Fourier Transform Infrared (FTIR) Spectroscopy. *J. Chem. Educ.* **2012**, *89*, 387–390.
- (39) Rasband, W. Download, National Institutes of Health. <https://imagej.nih.gov/ij/download.html> (accessed 2023-05-02).
- (40) Paul, D. R.; Barlow, J. W. Polymer blends (or alloys). *J. Macromol. Sci. Rev. Macromol. Chem. Phys.* **1980**, *C18* (1), 109–68.
- (41) Hikima, Y.; Morikawa, J.; Hashimoto, T. Imaging of Two-Dimensional Distribution of Molecular Orientation in Poly(Ethylene Oxide) Spherulite Using IR Spectrum and Birefringence. *Macromolecules* **2012**, *45*, 8356–8362.

(42) Han, T.; Gui, C.; Lam, J. W.; Jiang, M.; Xie, N.; Kwok, R. T.; Tang, B. Z. High-Contrast Visualization and Differentiation of Microphase Separation in Polymer Blends by Fluorescent Aie Probes. *Macromolecules* **2017**, *50*, 5807–5815.

(43) Krämer, G.; Griepentrog, M.; Bonaccorso, E.; Cappella, B. Study of Morphology and Mechanical Properties of Polystyrene–Polybutadiene Blends with Nanometre Resolution Using AFM and Force–Distance Curves. *Eur. Polym. J.* **2014**, *55*, 123–134.

(44) Raghavan, D.; Gu, X.; Nguyen, T.; Van Landingham, M.; Karim, A. Mapping Polymer Heterogeneity Using Atomic Force Microscopy Phase Imaging and Nanoscale Indentation. *Macromolecules* **2000**, *33* (7), 2573–2583.

(45) Tiganis, B.; Burn, L.; Davis, P.; Hill, A. Thermal Degradation of Acrylonitrile–Butadiene–Styrene (ABS) Blends. *Polym. Degrad. Stab.* **2002**, *76* (3), 425–34.